Published in final edited form as:
J Pharm Sci. 2009 September ; 98(9): 3290–3301. doi:10.1002/jps.21707.

Precipitation of a Monoclonal Antibody by Soluble Tungsten

Jared S. Bee[1], **Stephanie A. Nelson**[1], **Erwin Freund**[2], **John F. Carpenter**[3], and **Theodore W. Randolph**[1]

[1] Department of Chemical and Biological Engineering, University of Colorado, Boulder, Colorado 80309

[2] Drug Product & Device Development, Amgen Inc., Thousand Oaks, CA 91320

[3] Department of Pharmaceutical Sciences, University of Colorado Health Sciences Center, Denver, Colorado 80262

Abstract

Tungsten microparticles may be introduced into some pre-filled syringes during the creation of the needle hole. In turn, these microcontaminants may interact with protein therapeutics to produce visible particles. We found that soluble tungsten polyanions formed in acidic buffer below pH 6.0 can precipitate a monoclonal antibody within seconds. Soluble tungsten in pH 5.0 buffer at about 3 ppm was enough to cause precipitation of a mAb formulated at 0.02 mg/mL. The secondary structure of the protein was near-native in the collected precipitate. Our observations are consistent with the coagulation of a monoclonal antibody by tungsten polyanions. Tungsten-induced precipitation should only be a concern for proteins formulated below about pH 6.0 since tungsten polyanions are not formed at higher pHs. We speculate that the heterogenous nature of particle contamination within the poorly mixed syringe tip volume could mean that a specification for tungsten contamination based on the entire syringe volume is not appropriate. The potential potency of tungsten metal contamination is highlighted by the small number of particles that would be required to generate soluble tungsten levels needed to coagulate this antibody at pH 5.0.

Keywords

protein aggregation; microparticles; protein delivery; injectables; injectors; tungsten; monoclonal antibody; syringe; contamination; precipitation

INTRODUCTION

Aggregates of several different therapeutic protein products have caused severe immune responses in patients.1 Because of several documented cases where containers or delivery systems (e.g., IV tubing)2,3 caused protein aggregation,4 the compatibility of therapeutic protein products with containers and closures is drawing increasing attention from the biotechnology industry. Recent examples of protein instabilities related to containers include the formation of visible protein particles in at least two therapeutic products caused by tungsten particles in pre-filled syringes.5 Tungsten oxide vapor deposits in the syringe funnel area and tungsten particles are occasionally shed from the pins used to create the needle-mounting hole in pre-filled glass syringes as they age during usage.6

Correspondence to: Theodore W. Randolph (Telephone: 303-492-4776); (Theodore.Randolph@colorado.edu).

Cases such as these have prompted the FDA to classify container-closure changes as “high-risk” because of the possibility of severe patient immune responses to increased aggregation levels caused by the container-closure.5

To provide increased convenience for patients therapeutic proteins are increasingly packaged in pre-filled glass syringes. Commercial production of glass syringes generally requires the use of a heated wire to form the needle mount exit hole, and tungsten wires are used preferentially for this purpose because their high melting temperatures, mechanical stability, and low toxicity.6 Even so, during this process tungsten wires erode and vaporize, depositing minute amounts of tungsten-containing particulates on the wall in needle mount area of the syringe.6

Key aspects of tungsten and tungsten oxide chemistry have been described in detail by Lassner and Schubert.7 Here, we briefly summarize aspects of this chemistry of relevance to the syringe manufacturing process. During syringe manufacture a hot tungsten pin is used to create the needle exit hole. The temperature of the pin varies depending upon the exact process, but formation of syringes from borosilicate glass generally requires temperatures of 1000–1200°C.8 Tungsten metal begins to oxidize to tungsten oxide (WO_3) at about 400°C. Above 500°C the oxide layer cracks, and at 800°C the WO_3 starts to sublime.7 Therefore the oxidation of tungsten and vapor phase transport of sublimed WO_3 and deposition on cooler parts of the syringe are expected to contribute to the contamination process in addition to simple mechanical wearing of the pin. Also, it is known that when tungsten metal is dissolved in acidic solution (below about pH 6.0)9 it can form a variety polyanionic species such as paratungstate-A ($W_7O_{24}^{6-}$), paratungstate-B ($W_{12}0_{42}H_2^{10-}$), and metatungstate ($(H_2)W_{12}O_{40}^{6-}$).9 Thus, in prefilled syringes a protein product could potentially be exposed to particulates of tungsten metal and WO_3 as well as soluble polyanionic species of tungsten. It has been known since 1919 that addition of sodium tungstate, which could result in formation of soluble polyanionic species, causes precipitation of proteins from human blood.10

The purpose of this work was to investigate the effects of microparticles of tungsten metal, WO_3, and soluble sodium tungstate salt (Na_2WO_4) on the solution stability of a model monoclonal antibody. We investigated two possible mechanisms of protein particle formation. The first was that tungsten leached from metal or metal oxide microparticles could induce precipitation of a mAb. The second was that direct adsorption to microparticles could result in loss of soluble mAb. The amount of the three sources of tungsten required to cause antibody precipitation was determined in pH 5.0 buffer. The stability of the mAb formulation with respect to soluble tungsten was evaluated in buffers at pH 5.0, 5.5 and 6.0. The rate and extent of dissolution of soluble tungsten species leached from both tungsten metal and WO_3 microparticles was evaluated at pH 5.0. We characterized the secondary structure of the mAb in the precipitates formed by the interaction of the monoclonal antibody and soluble tungsten species, and compared them with the native-state secondary structure. The reversibility of formation of precipitates formed in pH 5.0 buffer was studied by resuspension in phosphate buffered saline (pH 7.4).

MATERIALS AND METHODS

Materials

The model monoclonal antibody (mAb) used in these studies was a humanized immunoglobulin-G1 (IgG1) antistreptavidin donated by Amgen Inc. (Thousand Oaks, CA). This mAb is not a commercial or development product. The IgG1 was obtained as a stock solution at 23 mg/mL in 10 mM sodium acetate and 5% sorbitol at pH 5.0 and stored at 4–8°C. The sorbitol was removed from the stock protein solution by dialysis before use. 10

mM sodium acetate, pH 5.0 ("buffer A") was used for all experiments except for precipitation studies as a function of pH and redissolution studies. For pH studies the mAb was dialyzed into two additional buffers: "buffer B" was 10 mM sodium acetate (pH 5.5); "buffer C" was 10 mM sodium phosphate with 150 mM sodium chloride (pH 6.0). The properties of the IgG1 mAb are as follows: molecular weight, M = 145 kDa (including 3 kDa glycosylation); UV extinction coefficient, ε = 1.586 mL/mg.cm; isoelectric point, pI = 8.7; and hydrodynamic diameter, D_h = 10.5 ± 0.5 nm. Tungsten microparticles (<10 micron, 99.99+% pure) were purchased from Sigma-Aldrich (St. Louis, MO) and used without further processing. The tungsten particle specific surface area was determined to be 0.27 ± 0.01 m^2/g (see Methods). Microparticles of WO_3 (ca. <20 micron, 99+% purity) also were purchased from Sigma-Aldrich (St. Louis, MO). The WO_3 microparticles were heated in air at 425°C for 4 hours before use, in order to remove any potential organic contamination. The WO_3 microparticle specific surface area was determined to be 0.67 m^2/g. Sodium tungstate (Na_2WO_4) used to prepare soluble tungsten was purchased from Sigma-Aldrich (St. Louis, MO). All other chemicals used were of reagent grade or higher quality.

Particle Surface Area Determination

Specific surface areas for particles were determined using nitrogen adsorption and Brunauer-Emmett-Teller (BET) isotherm analysis with an Autosorb 1C (Quantachrome Instruments, Boynton Beach, FL).

Soluble Tungsten Elemental Analysis

Solution tungsten levels above 0.1 ppm were determined using inductively coupled plasma optical emission spectrometry (ICP-OES) using an ARL 3410+ (Thermo Fisher Scientific, Inc., Waltham, MA). The ICP-OES detection limit for soluble tungsten was 0.1 ppm. To assay tungsten levels below 0.1 ppm, a PerkinElmer (Waltham, MA) Sciex ELAN® DRC-e inductively coupled plasma with a mass spectrometer detector (ICP-MS) was used. The ICP-MS detection limit for soluble tungsten was 0.4 ppb.

Protein and Soluble Aggregate Assays

Size exclusion chromatography (SEC) was used to quantify levels of mAb monomer and soluble aggregates. SEC was performed with a TSK-GEL G3000SW_{XL} column and SW guard column (Tosoh Bioscience LLC, Montgomeryville, PA). A 126 pump (Beckman Coulter Inc., Fullerton, CA), with a Waters 717 Plus autosampler (Waters Corp., Milford, MA) were used. The mobile phase consisted of 100 mM sodium phosphate, 300 mM sodium chloride, and 0.01% w/v sodium azide (pH 7.0), and the flow rate was 0.6 mL/min. Protein was detected using a Beckman Gold 166 UV detector at 280 nm.

Incubation of mAb with Suspensions of Microparticles of Tungsten Metal and in Solutions of Na_2WO_4 in Buffer A

A suspension of tungsten metal microparticles (10 mg/mL) in buffer A was stirred for 5 min. Then aliquots were removed and added to mAb in buffer in 1.7 mL polypropylene microcentifuge tubes to achieve the desired concentration of microparticles (0–9 mg/mL) and a constant 0.1 mg/mL mAb concentration, in a final sample volume of 0.5 mL. Samples were incubated at 4–8 °C for 5 min. After 5 min of incubation the samples were centrifuged (12,000 ×g at room temperature) for 30 min, and the supernatant was analyzed by SEC.

Because tungsten in acidic solution is known to form soluble polyanions9 we also performed additional incubations of mAb with the supernatant from a centrifuged suspension of tungsten metal microparticles and with soluble Na_2WO_4. A suspension of 10 mg/mL tungsten microparticles in buffer A was prepared and stirred for 5 min at room temperature.

A supernatant fraction was prepared by centrifuging the suspension at 12,000 ×g for 5 min. The supernatant was collected and recentrifuged for 30 min. The soluble tungsten content of the final supernatant was determined to be 25 ± 1 ppm using ICP-OES elemental analysis. The pH of the supernatant was measured as 5.09 and was not adjusted further because it was within 0.1 units of the desired pH. Various amounts of this supernatant were mixed with 50 μL of 1 mg/mL mAb and the appropriate volume of buffer A to create samples with soluble tungsten levels varying from 0–23 ppm at a constant mAb concentration of 0.1 mg/mL in a volume of 0.5 mL. Samples were incubated and analyzed as described above.

For incubations of Na_2WO_4 with 0.1 mg/mL mAb a 37 ppm stock solution of Na_2WO_4 in buffer A was used. Because the tungsten species in solution is very pH dependent9 we adjusted the pH back from 5.4 to 5.0 to maintain consistent solution conditions with the tungsten metal extract. Various amounts of the stock solution were mixed with mAb and buffer A to create samples with soluble tungsten levels varying from 0–33 ppm at a constant mAb concentration of 0.1 mg/mL. Samples were incubated and analyzed as described above.

To investigate the effect of mAb concentration on precipitation we repeated the incubation in Na_2WO_4 solutions with mAb at 0.02 mg/mL and 1.2 mg/mL. In these experiments, soluble tungsten levels ranged from 0–9 ppm and 0–129 ppm for incubations with 0.02 mg/mL and 1.2 mg/mL mAb, respectively. Samples were incubated and analyzed as described above.

In addition, to study the effects of a very high mAb concentration we added 15 μL of either a 18,400 ppm or a 184,000 ppm sodium tungstate solution to 185 μL of mAb at 131 mg/mL. The resulting mixtures contained 111 mg/mL mAb and either 2,800 ppm or 28,000 ppm of soluble tungsten. The 111 mg/mL mAb solution supernatants were diluted 10-fold twice in sequence for SEC analysis. Upon the initial 10-fold dilution, the 28,000 ppm tungstate-mAb preparations produced a large amount of voluminous white precipitate, although no precipitate was visible prior to dilution.

Incubation of mAb with Solutions of Na_2WO_4 as a Function of pH in Buffers A, B and C

Many mAbs currently marketed are formulated at pHs greater than 6.0 so we expect that polyanions of tungsten will not be present in these formulations and therefore not cause precipitation. In a review of mAb products currently marketed only 3 out of 23 were formulated below pH 6, although there may be other mAb products currently in development that have been evaluated for stability in lower pH formulations.11

To test this theory we performed the same incubation experiments of mAb at 0.1 mg/mL with Na_2WO_4 in buffer B (at pH 5.5) and buffer C (at pH 6.0) as was performed with mAb in buffer A (pH 5.0). The procedure used was the same as described above except that a stock solution of Na_2WO_4 was prepared in buffer B and buffer C at about 500 ppm soluble tungsten (the pH was adjusted as appropriate for each buffer).

Size Analysis of Soluble Tungsten Species Dissolved from Metal Microparticles

We used filtration to separate soluble tungsten species by size in a similar way to that described by Bednar *et al.* to evaluate the relative amount of large polyanions versus the smaller tungstate anion (WO_4^{2-}).12 A tungsten-containing supernatant was prepared from metal microparticles as described above, and the total soluble tungsten measured by ICP-OES as described above. Aliquots of the tungsten-containing supernatant were filtered with both 3,000 (~1.7 nm) and 10,000 (~2.9 nm) nominal molecular weight limit centrifugal filtration devices and the filtrate analyzed for soluble tungsten content. The filtration devices used were Ultracel® brand YM-3 and YM-10 devices (Millipore, Bedford, MA): the

approximate relationship between size in nm and molecular weight cutoff was provided by Millipore. The tungsten in each filtrate was compared to the total soluble tungsten level, and used to determine the relative amounts of large and small tungsten species in solution.

Reversibility of mAb Precipitate Formation

A precipitate was formed by incubation of 0.1 mg/mL mAb with 33 ppm soluble Na_2WO_4 for 5 min at 4–8°C. To collect the precipitate, 0.5 mL samples were centrifuged for 5 minutes at 12,000 ×g and the supernatant was removed. Precipitation was quantitative, with no soluble mAb detectable by SEC (see above) in the supernatant. Reversibility of the mAb precipitation was assessed by resuspension of the precipitate either in 1.5 mL of acetate buffer A (pH 5.0) or in 0.5 mL of phosphate buffered saline (137 mM NaCl, 10 mM phosphate and 2.7 mM KCl at pH 7.4, PBS). This test was designed to find whether the precipitate would redissolve following dilution or by resuspension in a solution representative of extracellular fluid (PBS). SEC was used to assay the recovery of protein after the reversibility tests.

Precipitate Tungsten Content Analysis

To determine how much tungsten was contained in the precipitate formed in the reversibility study (see above) the experiment was performed with 10 mL samples, and the tungsten levels in the supernatant after precipitation and re-dissolution in PBS were measured and compared.

Adsorption of mAb to WO_3

The amount of mAb adsorbed to WO_3 microparticles was determined by depletion of protein from solution after mixing with particles and performing a mass balance. A stock 454 mg/mL suspension of WO_3 particles in buffer A was prepared. Samples were prepared by mixing buffer A, the microparticle suspension, and a stock mAb solution to yield samples with a constant final protein concentration of 0.156 mg/mL in a total volume of 0.5 mL, and a range of microparticle concentrations. The solutions were incubated at 4–8°C for 30 min with mixing by end-over-end rotation in 1.7 mL polypropylene microcentrifuge tubes at 8 rotations per minute. Samples were then centrifuged for 30 min at 12,000 ×g, and the supernatant was assayed for protein content by SEC. The fraction of mAb monomer remaining in solution was plotted versus the microparticle surface area added per milligram of protein and extrapolated to the x-axis intercept to find the apparent surface area occupied per mg mAb adsorbed on WO_3 microparticles. Experiments were performed in triplicate.

Tungsten Dissolution from Microparticles

The rate and extent of dissolution of tungsten metal and WO_3 microparticles was found by measuring the soluble tungsten levels in stirred particle dispersions over time. Two separate experiments were performed: one experiment simulated extraction into a formulation buffer A (using 10 mM sodium acetate at pH 5.0), and another experiment evaluated a dissolution procedure that potentially could be used to remove tungsten deposits from glass syringes using 0.1 M NaOH with 3% w/v H_2O_2 to dissolve microparticles. In both studies, enough tungsten or WO_3 microparticles were added to 1 L of the dissolution medium to give about 100 ppm of total tungsten. The suspensions were stirred using a Teflon® coated stir bar. 1.0 mL aliquots were removed at various time points, centrifuged, and the supernatant analyzed for soluble tungsten. The pelleted solid was returned to the original suspension. No correction was applied for the removal of each 1 mL aliquot as it is was only 0.1% of the total volume of solution. The temperature was about 23°C for these studies, except for the WO_3 washing procedure, where the dispersion temperature was increased to 95°C after 100 min because particles were still observed in the medium.

mAb Secondary Structure Analysis with Infrared Spectroscopy

The secondary structures of the native, soluble protein and precipitated protein were analyzed using infrared spectroscopy. Spectra were acquired on a Bomem MB-series spectrometer (PQ, Canada). A BioCell (BioTools Inc., Jupiter, FL) with CaF_2 windows and a 6.5 μm path length was used to collect 128 single-beam transmission scans at 4 cm^{-1} resolution. The second derivative was calculated with a 7 or 9 point Savitsky-Golay function depending upon the data quality. The derivative spectra were then baseline corrected, area-normalized, offset corrected, and interpolated with a 2× fast Fourier transform function. Spectral quality was assessed according to previously published specifications.13 Triplicate samples of the reference protein, the precipitate produced with supernatant from tungsten microparticle suspensions (immediate analysis), and precipitate produced with Na_2WO_4 (and stored for 5 days at 4–8°C) were analyzed.

RESULTS

Incubation of mAb with Suspensions of Microparticles of Tungsten Metal in Buffer A

Incubation of mAb at 0.1 mg/mL with tungsten metal microparticles in buffer A resulted in rapid, quantitative loss of protein from solution. The tungsten levels required to effect precipitation (Figure 1) were far lower than would be predicted by simple monolayer adsorption to the surface of the tungsten particles. Only 9 mg/mL of tungsten microparticles were required to remove almost all of the mAb from solution. We calculated that if the mAb were adsorbed to tungsten particles in a hexagonally packed monolayer it would have a theoretical coverage footprint of 0.4 m^2 of surface area per mg of mAb (about 2.5 mg/m^2 loading). For suspensions containing 9 mg/mL tungsten microparticles, the surface area was 0.0025 m^2 of surface area per mg of mAb. This represents only enough area to adsorb 0.6% of the mAb as a monolayer.

Incubation of mAb with the Supernatant from Suspensions of Tungsten Metal Microparticles and in Solutions of Na_2WO_4 in Buffer A

To test whether soluble tungsten species derived from microparticles could cause mAb precipitation, we added tungsten solutions in buffer A prepared from microparticles (see Methods) to mAb. Figure 2 shows that the threshold level of soluble tungsten needed to initiate precipitatation of protein within the 5 minute incubation period from solutions containing 0.1 mg/mL mAb was about 5 ppm in buffer A; precipitation was essentially complete in solutions containing 20 ppm soluble tungsten. The precipitation behavior was independent of the source of the soluble tungsten; dissolved tungsten from metal microparticles and solutions of Na_2WO_4 yielded essentially identical results. These observations suggest that soluble tungsten species, and not direct protein-microparticle interactions are responsible for precipitation of mAb in the presence of tungsten metal microparticles. After precipitates were removed from samples by centrifugation, the remaining supernatants were analyzed by SEC and found to contain no increase in soluble oligomer levels.

We studied the effect of mAb concentration on the threshold concentration of soluble tungsten needed for mAb precipitation and also how the extent of mAb precipitation was dependent upon Na_2WO_4 concentration. Initial precipitation from 0.02 mg/mL mAb solutions in buffer A occurred at around 3 ppm Na_2WO_4 (Figure 2). Precipitation of mAb from solutions containing 1.2 mg/mL mAb required greater Na_2WO_4 levels to cause the same percentage mAb precipitation.

We also conducted experiments with very high concentration mAb (131 mg/mL), which reflect the levels of protein often contained in therapeutic protein formulations. The

dependence of the coagulation process on mixing was clearly evident. When 18,400 ppm Na_2WO_4 was added to to 131 mg/mL mAb (yielding 2,800 ppm tungsten and 111 mg/mL mAb) a voluminous white plume of precipitate was formed at the pipette tip. Approximately 10 seconds after the initial injection, turbidity resulting from the precipitate diminished. This contrasts with observations made in the experiments with lower mAb concentrations, where the turbidity due to precipitation remained visible. After mixing and centrifugation the appearance of the pellet was variable across triplicate samples: precipitated mAb was either not visible or translucent in appearance. After the 100× dilution of the supernatant required for SEC analysis, a variable amount of the mAb was recovered (98 ± 14 %).

In other experiments with 28,000 ppm Na_2WO_4 and 111 mg/mL mAb the initial precipitate also became less visible after mixing. After centrifugation, no pellet was observed. However, during the first 10× dilution of the supernatant for SEC analysis, a white precipitate was observed throughout the sample volume. After the second 10× dilution and centrifugation, all of the mAb was removed from the supernatant.

Incubation of mAb with Solutions of Na_2WO_4 as a Function of pH in Buffers A, B and C

The soluble Na_2WO_4 threshold concentrations for inducing mAb precipitation from formulations containing 0.1 mg/mL mAb are shown as a function of pH in Figure 3. The threshold increases sharply, increasing from about 5 ppm in buffer A at pH 5.0 to about 30 ppm in buffer B at pH 5.5. No precipitation was measured, even for soluble tungsten levels of over 200 ppm, in buffer C at pH 6.0. This data is consistent with the fact that tungsten polyanions do not form above about pH 6.0.9

Infrared Spectroscopic Analysis of mAb Secondary Structure

The second derivative IR spectrum of precipitate induced by soluble tungsten dissolved from tungsten microparticles is shown in Figure 4. Comparison of the spectrum of the precipitate with that for the native, soluble mAb shows that the precipitate contains mAb with a native secondary structure. The maximum in the amide-I band at 1637 cm^{-1} is characteristic of the β-sheet content of immunoglobulin proteins.13 There is a small decrease in the peak at about 1614 cm^{-1} in the precipitate compared with that for the native protein. This peak is normally attributed to either aggregated strands,14 or side-chain interactions.15 Since it decreases in the precipitate it is probably due to a change in the spectra of the side chain interactions when this mAb is associated with tungsten polyanions. The spectrum of the precipitate produced by addition of Na_2WO_4 and stored for 5 days at 4–8°C (not shown) was essentially identical to the spectrum of the precipitate described above. Thus, the tungsten-induced precipitates contain mAb with native secondary structure.

Reversibility of Precipitate Formation

The precipitate formed by interaction of the mAb with Na_2WO_4 was reversible when immediately resuspended in PBS but not when diluted by a factor of 3 in the original pH 5.0 acetate buffer A. Upon addition of PBS, the precipitate appeared by visual inspection to dissolve within a few seconds.

The recovery of total soluble mAb after the precipitate was dissolved in PBS was 97%, although the percentage of soluble dimers and oligomers increased from 2.3% in the solution prior to precipitation to 7.8%. The peak corresponding to oligomers for the redissolved mAb appeared at the same retention time as expected for a dimer, but with at least 2 small unresolved shoulders at shorter retention time confirming the presence of larger oligomers. We repeated the PBS dissolution study on a precipitate that was stored for 5 days at 4–8°C. In this case only 91% of the total protein was recovered and it contained 5.6% soluble dimer/oligomers.

Analysis of Tungsten Content in Precipitates

The molar ratio of tungsten to mAb in the precipitate was 62:1, as determined from ICP-OES measurements and mass balances.

Size Analysis of Soluble Tungsten Species

The total tungsten soluble extract content in the filtration study was 4.9 ± 0.1 ppm. The filtrates recovered using 10,000 and 3,000 molecular weight cutoff membranes contained 4.76 ± 0.01 ppm and 2 ± 1 ppm of soluble tungsten respectively. Filtration through a 3,000 molecular weight cutoff (~1.7 nm) membrane removed about half of the soluble tungsten. The 10,000 molecular weight cutoff (~2.9 nm) membrane did not remove a significant amount of tungsten from solution. Since the membrane material was the same for the two filters, and most of the tungsten passed through the larger membrane, we can rule out any significant specific adsorption of smaller soluble tungsten species to the membrane material itself. Thus, it appears that approximately half of the tungsten present in the initial solution is present as polyanions that can be removed by filtration through a 3,000 molecular weight cutoff membrane but not by a 10,000 molecular weight cutoff membrane. The bare paratungstate-A anion size is on the order of 1 nm as estimated from the crystal structure,16 although the hydration of the paratungstate-A anion should make it somewhat larger in solution. The total level of tungsten in this study was consistent with the value of 9 ppm previously reported for polyanions species to be dominant in solution.17

Tungsten Extraction and Dissolution Study

Figure 5 shows that the relative rate and extent of dissolution of tungsten from metal microparticles is much greater than from WO_3 microparticles in sodium acetate buffer A (pH 5.0): a suspension of tungsten metal particles (100 ppm total tungsten) yielded 12 ppm of soluble tungsten after 7 days. In contrast, WO_3 microparticles (also 100 ppm total tungsten) appeared to reach an equilibrium concentration of about 1 ppm soluble tungsten after 5 days. Consistent with the equilibrium interpretation, WO_3 crystals were observed adhered to the glass surface after several days. Because the solubility of tungsten species can vary by pH7,9,18 (for example, polyanions are not formed above ~ pH 6) we also expect the rate and extent of tungsten dissolution from the metal and WO_3 to vary depending upon the exact solution conditions.

In the study of a potential syringe washing protocol (using 0.1 M NaOH and 3% w/v H_2O_2), microparticles (100 ppm total tungsten) of tungsten metal or WO_3 were suspended in the washing solution. Within 20 min at 23°C, 81 ppm of the tungsten metal dissolved, but only 10 ppm of WO_3 dissolved after 100 min at 23°C. Heating of the WO_3 microparticle suspension to about 95°C for 45 minutes resulted in complete dissolution

Adsorption of mAb to WO_3 microparticles

Because the amount of tungsten dissolved from WO_3 microparticles was less than 3 ppm, we did not expect soluble tungsten from WO_3 microparticles to precipitate this mAb. Consistent with this expectation, we measured adsorption of the mAb to WO_3 in amounts consistent with the formation of a simple monolayer. The titration isotherm of this mAb on WO_3 is shown in Figure 6. The x-axis intercept of 0.98 ± 0.07 m^2 per mg of mAb represents the apparent adsorption footprint of this mAb on WO_3. The observed value is larger than the prediction of 0.4 m^2 per mg of mAb for hexagonal close packing (hcp) by calculating the geometric packing of 10.5 nm discs on a surface. The Random Sequential Adsorption19 (RSA) model predicts a hard-disc footprint of 0.67 m^2 per mg of mAb, which is closer to the observed experimental value than the hcp prediction. The characteristic hard-disc packing surface coverage is 55% in the RSA model because the RSA model includes the inefficiency

of random packing on the surface.19 The observed footprint could be larger than the RSA prediction because of charge repulsion between mAb molecules as the surface fills,20 or because of unfolding of the mAb on the microparticle surface. No increase in soluble aggregate levels was detected by SEC in the 30 min adsorption study. The level of WO_3 particles necessary to remove the mAb from solution is consistent with a simple monolayer adsorption process.

DISCUSSION

Our experimental results showed that tungsten metal microparticles can dissolve in acidic buffers below about pH 6 to produce soluble tungsten polyanions that can precipitate a mAb at tungsten levels of 3 ppm or greater. We confirmed the presence of tungsten polyanions in the tungsten metal extract by using filtration to remove larger polyanions. Soluble tungsten was confirmed as the cause of mAb loss because incubations with the metal particle suspension supernatant and completely soluble Na_2WO_4 gave almost identical results for the same soluble tungsten levels. The infrared spectrum of the collected precipitate showed that the mAb retained its near-native secondary structure in the precipitate. The precipitate could be redissolved in PBS but the released mAb had markedly increased aggregate levels.

In acidic solutions below about pH 6 tungsten forms polyanion species like paratungstate-A ($W_7O_{24}^{6-}$), paratungstate-B ($W_{12}0_{42}H_2^{10-}$), and metatungstate ($(H_2)W_{12}O_{40}^{6-}$).9 The exact composition of the solution depends upon the tungsten concentration, pH, and age of the solution.9 At short times following dissolution, paratungstate-A is the dominant species in solutions with tungsten concentrations of 9 ppm and above and over hours to days other tungsten polyanionic species are formed.9,17 In our experiments we found that about half of the tungsten was in the form of polyanions at 5 ppm at pH 5.0. The paratungstate-A anion has a compact cluster-like structure,16 and because it has a 6 charge we propose that electrostatic interactions with the mAb could explain the very fast mAb precipitations we observed. Elemental analysis of the redissolved precipitate solution showed that the precipitate contained tungsten and protein in a molar ratio of 62:1 (equivalent to 1:13 tungsten-to-mAb on a mass basis). At short times after dissolution, paratungstate-A ($W_7O_{24}^{6-}$) is the major tungsten polyanion in acidic solution,9 so, the molar ratio of paratungstate-A to mAb in the precipitate was about 9:1. Because the mAb has a predicted charge of 60+ under these solution conditions, this ratio supports our interpretation that mAb co-precipitates with paratungstate-A resulting in charge-neutrality. Because WO_3 microparticles only dissolved to an equilibrium solution tungsten level of about 1 ppm, precipitation by tungsten polyanions in incubations of mAb with WO_3 was not observed. Instead, WO_3 depleted mAb from suspensions at levels consistent with a simple adsorption process.

The precipitation of mAb by tungsten polyanions was dependent upon the tungsten and mAb concentrations as well as the pH of the formulation. The lowest observed concentration of tungsten that could precipitate the mAb was 3 ppm for 0.02 mg/mL mAb solutions at pH 5.0. Assuming that paratungstate-A is the predominant tungsten species in solution, and that at 5 ppm tungsten about half of the tungsten was present as polyanions, the precipitation threshold occurred at a ratio of paratungstate-A to mAb of about 8:1. Given that the theoretical net charge of the mAb is about 60+ at pH 5.0, this ratio is consistent with the 10:1 paratungstate-A to mAb ratio expected for charge neutralization.

More soluble tungsten was needed to precipitate the mAb from solutions containing higher protein concentration. In a formulation at pH 5.0, the precipitation threshold concentration of tungsten was 3 ppm at 0.02 mg/mL mAb, 5 ppm at 0.1 mg/mL mAb, and over 11 ppm at 1.2 mg/mL mAb. Measurement of threshold concentration of tungsten needed to cause

precipitation was limited by the ability of the SEC assay to measure smaller relative mAb losses from high concentration mAb solutions at very low ppm tungsten levels. The paratungstate-A-to-mAb molar ratio required for complete precipitation was 50:1 for 0.02 mg/mL mAb (9 ppm W), 20:1 for 0.1 mg/mL mAb (18 ppm W), and about 11:1 for 1.2 mg/mL mAb (130 ppm). The lower polyanion content in low ppm tungstate solutions could partly account for the higher tungsten-to-mAb ratios needed to completely precipitate the mAb at 0.02 mg/mL.

In our experiments at very high mAb concentration (>100 mg/mL) we observed the formation of a precipitate as the tungsten was added to the mAb which then could be seen to diminish upon further mixing. Repeated experiments demonstrated that the mAb precipitation was small and highly variable even though we observed visible particles initially. Our experimental observations suggest that the precipitation of mAb by tungsten polyanions is dependent upon a minimum threshold level of tungsten polyanions (3 ppm in pH 5.0 buffer), the ratio of tungsten to mAb, and the mixing of tungsten with mAb. We found that the pH of the formulation is also critical: at pH 6.0, no coagulation of our mAb was observed even at soluble tungsten levels above 200 ppm, which is consistent with the fact that tungsten does not form polyanions above about pH 6.0.9 This means that it is unlikely that this mechanism is occurring in mAb products formulated above pH 6.0.

These data and observations are consistent with a coagulation mechanism for mAb precipitation by tungsten polyanions in acidic formulations. Coagulation refers to the precipitation of a colloid after destabilization of the colloidal suspension with counter-ions of opposite charge.21–23 For simple, “indifferent” counter-ions (like Na^+) the colloidal destabilization is a result of the screening of electrostatic repulsion between the colloids by the counter-ions. 21,22 This is the basis of Deryagin-Landau and Verwey-Overbeek (DVLO) theory, where colloidal stability is a result of the balance between attractive dispersion forces and repulsive electrostatic forces.21,22 In the case of electrostatic screening by indifferent counter-ions there is a critical coagulation concentration (CCC) of counter-ions that results in enough screening to reduce the repulsive barrier to coagulation between colloids to zero.21,22 Because indifferent counter-ions destabilize the colloid by screening of electrostatic repulsion forces, the CCC is not dependent upon the colloid concentration itself.21,22 In our case we expect more can also complicated behavior. Polynuclear counter-ions (like paratungstate-A, $W_7O_{24}^{6-}$) physically adsorb to the colloid (mAb) surface and therefore also change the surface potential of the colloid.19 Because we hypothesize that paratungstate-A can bind to the mAb, we expect it can reduce the net charge of the mAb in addition to screening the electrostatic repulsion between mAbs.19 Furthermore, polyanionic species that bind to the surface of proteins may form bridges between protein molecules, which lead to large, insoluble tungsten-protein assemblies.

Coagulation can be characterized by regions of stability and instability defined by experimental critical coagulation concentrations and critical stabilization concentrations that now also depend upon other parameters, such as the concentration of counter-ion and pH. 21–23 The critical stabilization concentration occurs when the amount of counter-ion is “overdosed” so that enough adsorbs to the colloid to impart an opposite surface charge resulting in re-stabilization of the colloid.21–23 To complicate matters further, the rate and order of addition of coagulant, mixing intensity, and mixing time can each impact experimental observations.21–23

Coagulation as a process explains some of our variable experimental results because it is highly dependent upon factors like temperature, coagulant species, order of addition, pH, and rate of mixing.21–23 In our system we hypothesize that there is no coagulation of the colloid (mAb) until the coagulant (tungsten polyanions) concentration reaches the critical

coagulation concentration of ca. 3 ppm, whereupon the colloid (mAb) is precipitated by charge neutralization.23 As the coagulant (tungsten polyanions) concentration is increased further, charge reversal23 could restabilize the mAb colloid, resulting in a reversal of the coagulation process, as noted in the experiments using high mAb concentrations. Poor mixing in the high concentration experiments we performed could have resulted in charge reversal and stabilization of the mAb without efficient coagulation occurring.21–23 This interpretation is also supported by our observation that coagulation did not occur in the mAb formulated at pH 6.0, and that the precipitate formed from mAb formulated at pH 5.0 could be redissolved in PBS. The increased pH of 7.4 will both reduce the positive charge on the mAb and also cause tungsten polyanions to form simple WO_4^{2-} anions and therefore break apart the precipitate. Extensive experimentation would be required to completely characterize the coagulation process of this mAb. However, many of the effects that we have observed reflect protein aggregation behavior that has been observed in actual syringe systems.

We suggest that under some conditions particles may form by coagulation of mAb with only 3 ppm of soluble tungsten without a measurable loss of monomeric mAb. This phenomenon could account for the appearance of visible proteinaceous particles that constitute a small fraction of the total protein. For example, in our experiments precipitates containing only 50 μg/mL of protein appeared as highly visible white particles, which would represent only 0.05% of the protein in 1 mL of a 100 mg/mL formulation. Because of the complex nature of coagulation processes, tungsten polyanions could bind with mAb to form many sub-visible particles or a few large visible particles.

Physicians are trained to discard any product with visible particles unless there are specific instructions for filtering before, or during, parenteral administration.25 Of course, this still leaves the possibility that sub-visible particles could be present in the injection administered to the patient. There are many factors in a real pre-filled syringe environment that could potentially change the rate and extent of mAb-polyanion interactions and also the visual appearance of any coagulated particles formed. A prudent approach may be to base any tungsten contamination specifications on the lowest level that could potentially cause a product quality issue.

After a tungsten pin is used to make the needle hole in syringes, residual tungsten deposits or particles may be present in the tip of the syringe. Tungsten deposited in the syringe may exist as either the metal or oxide. Coagulation of mAb will depend upon the rate and extent that soluble tungsten species are leached into the formulation and mix with protein molecules. Tungsten metal leaches enough soluble tungsten to cause mAb coagulation, but the WO_3 solubility of about 1 ppm appears to be too low to cause mAb precipitation by the polyanion coagulation mechanism. However, some tungsten oxides and polyanions may also foster protein oxidation and subsequent aggregation, an effect not explored in this study.

Thus, if a mixture of tungsten metal and tungsten oxides is present, any quantitative extraction or washing procedure should be able to remove both types of contamination. A hot hydroxide/peroxide mixture was a good dissolution medium for both W and WO_3, but we did not evaluate how it could impact the quality of pharmaceutical-grade glass.

In the needle mount area of syringes, there is a small (<5 μL) funnel volume where the needle is sealed that may not be well-wetted or well-mixed with the rest of the product.6 We speculate that tungsten contamination near the needle tip may not necessarily become a problem until the syringe undergoes some additional mechanical stress. External factors such as vibration or agitation caused by ground and air transportation may increase the speed of dissolution of tungsten metal particles and the enhance mixing of product between

the tip funnel and main body of the syringe. This situation has implications for the testing and specification setting for tungsten contamination levels. Our observations were that the concentrations and relative amounts of tungsten and mAb, and the amount of mixing, resulted in different measurable mAb losses by SEC assay. At 0.02 mg/mL mAb 3 ppm could cause coagulation. At higher mAb concentrations more tungsten was needed in order to cause a mAb loss greater than the variability of the SEC assay. If a local tungsten concentration in the syringe tip greater than 3 ppm can cause precipitation of the mAb, then a specification based on tungsten levels in the entire syringe volume may not be proper. For example, if the fill volume of a syringe is 0.5 mL and the tip funnel volume is about 5μL, then the local tungsten concentration could be up to 100 times higher in the tip funnel if all the contamination is localized there. Furthermore, only one to two 10-μm tungsten particles would be needed to generate a 3 ppm soluble contamination level in the 5μL syringe neck area, assuming complete dissolution. Even if we consider the entire syringe volume, only ~ 150 particles would be sufficient to generate 3 ppm soluble tungsten. The USP <788> (United States Pharmacopoeia, 2007) requires that parenterals remain free from visible particulates, and contain fewer than 6000 particles ≥10 μm and fewer than 600 particles ≥25 μm for small-volume injections.

Acknowledgments

Funding for this work was provided by the Graduate Assistantship in Areas of National Need (GAANN) program, the NIH Leadership in Pharmaceutical Biotechnology program (NIH T32 GM008732), the NIH (NIH NIBIB Grant 1 R01 EB006006-01), and Amgen Inc. We had particularly useful discussions with following people at Amgen: Danny Chou, Jennifer L. Stevenson, Koustuv Chatterjee, Robert Platz, Sampathkumar Krishan, and Linda Narhi. Thanks to Fredrick G. Luiszer for his help in performing the tungsten analyses.

Abbreviations

mAb	monoclonal antibody
SEC	size exclusion chromatography
UV	ultraviolet

References

1. Schellekens H. Immunogenicity of therapeutic proteins: Clinical implications and future prospects. Clinical Therapeutics. 2002; 24(11):1720–1740. [PubMed: 12501870]
2. Mcleod, Walker; Zheng, Hayward. Loss of factor VIII activity during storage in PVC containers due to adsorption. Haemophilia Haemophilia J1 - Haemophilia. 2000; 6(2):89.
3. Tzannis ST, Hrushesky WJM, Wood PA, Przybycien TM. Adsorption of a formulated protein on a drug delivery device surface. Journal of Colloid and Interface Science. 1997; 189(2):216–228.
4. Sharma B. Immunogenicity of therapeutic proteins. Part 2: Impact of container closures. Biotechnology Advances. 2007; 25(3):318–324. [PubMed: 17337336]
5. Rosenberg AS. Effects of protein aggregates: An immunologic perspective. Aaps Journal. 2006; 8(3):E501–E507. [PubMed: 17025268]
6. Swift, R.; Nashed-Samuel, Y.; Liu, W.; Narhi, L.; Davis, J. Tungsten, prefilled syringes and protein aggregation. 2007 ACS Meeting; Boston, MA. 2007. (BIOT 15)
7. Lassner, E.; Schubert, WD. Tungsten: Properties, Chemistry, Technology of the Element, Alloys, and Chemical Compounds. 1. New York: Kluwer Academic/Plenum Publishers; 1999.
8. Fries, A.; Schonknecht, T. Controlling the Alkali Release in Glass Based Prefillable Syringes. Poster Session: AAPS Meeting 2007; 2007.
9. Pope, MT. Heteropoly and Isopoly Oxometalates. ed. New York: Springer-Verlag; 1983.
10. Folin O, Wu H. A SYSTEM OF BLOOD ANALYSIS. J Biol Chem. 1919; 38(1):81–110.

11. Wang W, Singh S, Zeng DL, King K, Nema S. Antibody structure, instability, and formulation. Journal of Pharmaceutical Sciences. 2007; 96(1):1–26. [PubMed: 16998873]
12. Bednar AJ, Mirecki JE, Inouye LS, Winfield LE, Larson SL, Ringelberg DB. The determination of tungsten, molybdenum, and phosphorus oxyanions by high performance liquid chromatography inductively coupled plasma mass spectrometery. Talanta Special Issue on China-Japan-Korea Environmental Analysis - C-J-K Environmental 2006. 2007; 72(5):1828–1832.
13. Dong A, Huang P, Caughey WS. Protein secondary structures in water from second-derivative amide I infrared spectra. Biochemistry. 1990; 29(13):3303–3308. [PubMed: 2159334]
14. Jackson M, Mantsch HH. The Use and Misuse of Ftir Spectroscopy in the Determination of Protein-Structure. Critical Reviews in Biochemistry and Molecular Biology. 1995; 30(2):95–120. [PubMed: 7656562]
15. Fu FN, Deoliveira DB, Trumble WR, Sarkar HK, Singh BR. Secondary Structure Estimation of Proteins Using the Amide-Iii Region of Fourier-Transform Infrared-Spectroscopy - Application to Analyze Calcium Binding-Induced Structural-Changes in Calsequestrin. Applied Spectroscopy. 1994; 48(11):1432–1441.
16. Burtseva KG, Chernaya TS, Sirota MI. Determination of the crystal and molecular structure of sodium paratungstate. Soviet Physics Dolklady. 1978; 23(11):784–786.
17. Ng KYS, Gulari E. Spectroscopic and scattering investigation of isopoly-molybdate and tungstate solutions. Polyhedron. 1984; 3(8):1001–1011.
18. Dermatas D, Braida W, Christodoulatos C, Strigul N, Panikov N, Los M, Larson S. Solubility, sorption, and soil respiration effects of tungsten and tungsten alloys. Environmental Forensics. 2004; 5(1):5–13.
19. Evans JW. Random and Cooperative Sequential Adsorption. Reviews of Modern Physics. 1993; 65(4):1281–1329.
20. Oberholzer MR, Stankovich JM, Carnie SL, Chan DYC, Lenhoff AM. 2-D and 3-D interactions in random sequential adsorption of charged particles. Journal of Colloid and Interface Science. 1997; 194(1):138–153. [PubMed: 9367593]
21. Morrison, ID.; Ross, S. Colloidal Dispersions: Suspensions, Emulsions, and Foams. ed. New York: John Wiley and Sons, Inc; 2002.
22. Shaw, DJ. Introduction to colloid and surface chemistry. 4. Oxford: Butterworth-Heinemann Ltd; 1991.
23. Gregory, J. Particles in water: properties and processes. ed. New York: Taylor and Francis; 2006.
24. Jiang Y, Nashed-Samuel Y, Li C, Liu W, Pollastrini J, Mallard D, Wen Z, Fujimori K, Pallitto M, Donahue L, Chu G, Torraca G, Vance A, Mire-Sluis A, Freund E, Davis J, Narhi L. Tungsten-induced Protein Aggregation II: Solution Behavior. Journal of Pharmaceutical Sciences. 2008 Submitted.
25. Sifton, DW., editor. Physicians' desk reference. 56. Montvale, NJ: Medical Economics; 2002.

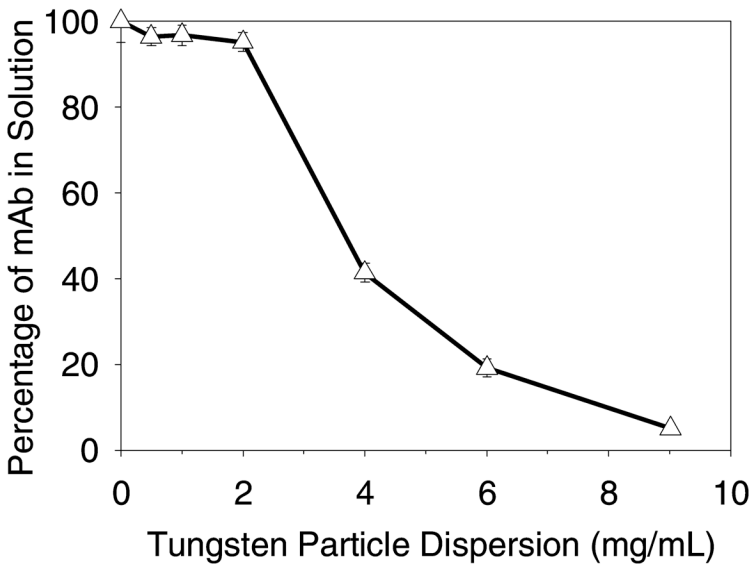

Figure 1.
Loss of soluble mAb as a function of amount of added tungsten microparticles. Data points are mean ±SD for separate triplicate samples. Error bars may be obscured by symbols.

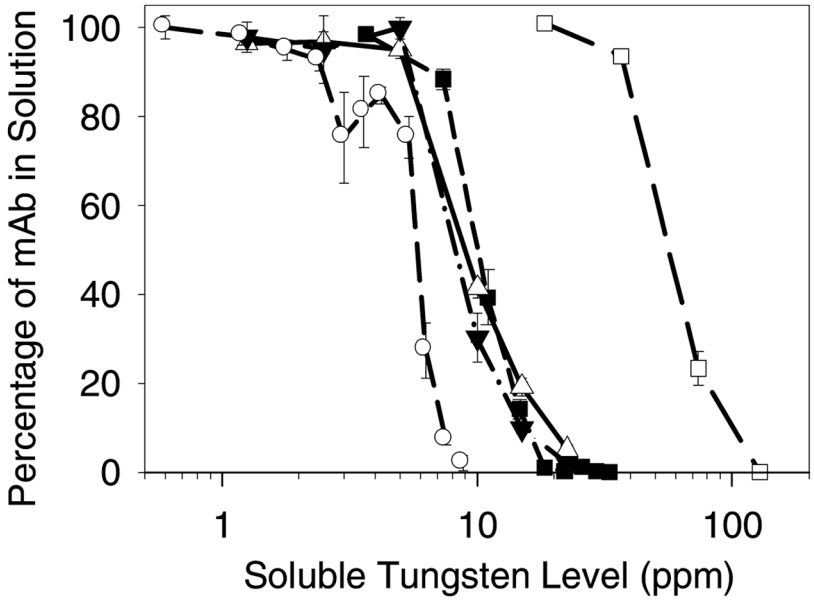

Figure 2.

Precipitation of mAb with soluble tungsten in buffer A (pH 5.0). Legend: tungsten particle suspension and 0.1 mg/mL mAb (▲); supernatant from tungsten particle suspension and 0.1 mg/mL mAb (▼;); Na_2WO_4 preparation and 0.1 mg/mL mAb (■); Na_2WO_4 preparation and 0.02 mg/mL mAb (○); Na_2WO_4 preparation and 1.2 mg/mL mAb (□). Data points are mean ±SD for separate triplicate samples. Error bars may be obscured by symbols.

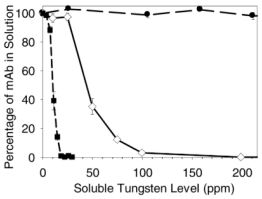

Figure 3.

Precipitation of mAb with soluble Na_2WO_4 as a function of pH. The mAb concentration was 0.1 mg/mL for all samples. Legend: mAb in buffer A at pH 5.0 (■); mAb in buffer B at pH 5.5 (◇); mAb in buffer C at pH 6.0 (●). Data points are mean ±SD for separate triplicate samples. Error bars may be obscured by symbols.

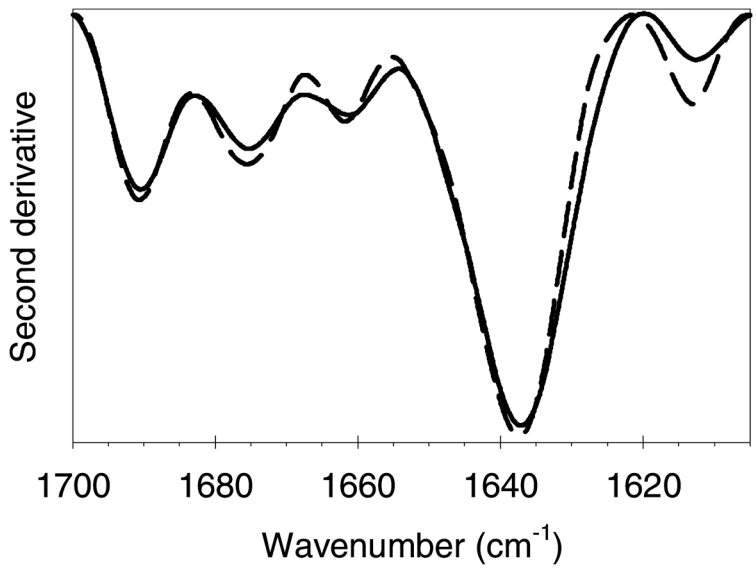

Figure 4.
Second-derivative transmission infrared spectra of the white precipitate formed by incubation of mAb with clarified tungsten metal particle extract. Representative spectra from three replicates are shown. Reproducibility was found to be very good, with near-overlay of the replicates. Legend: white precipitate, solid line; reference native mAb at 23 mg/mL, medium dashed line.

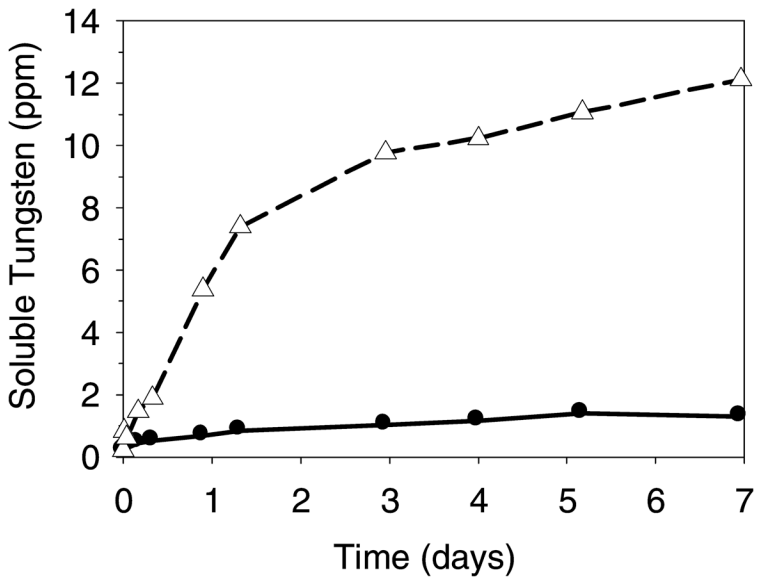

Figure 5.

Dissolution of soluble tungsten from tungsten metal microparticles and WO_3 microparticles in buffer A (10 mM sodium acetate buffer at pH 5.0) where 100 ppm total tungsten was added in both cases. Legend: dissolution from tungsten metal microparticles, open triangles and short dash line (▲); dissolution from WO_3 microparticles, solid circles and solid line (●). Data points are for single samples.

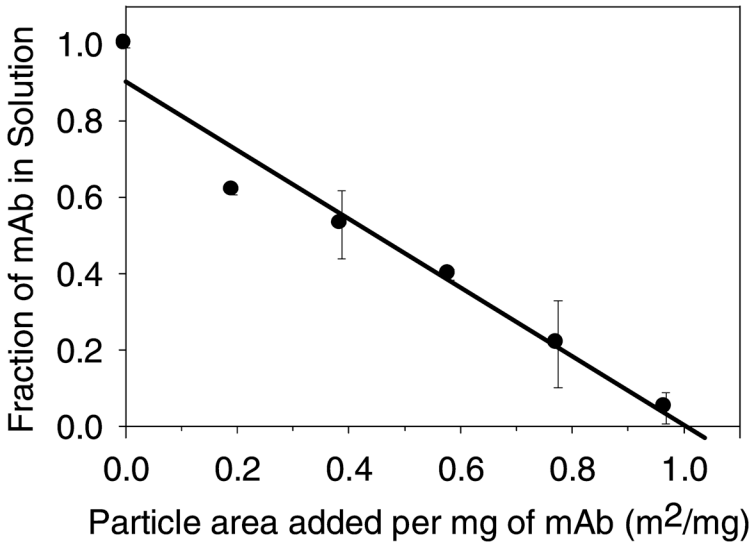

Figure 6.
Titration isotherm of mAb adsorption onto WO_3 particles. Data points are mean ±SD for separate triplicate samples. Error bars may be obscured by symbols.